



## Preparation of Nanostructured $\text{Li}_2\text{MnO}_3$ Cathode Materials by Single-Step Hydrothermal Method

G. R. Liu\*, S.C. Zhang†, X. X. Lu, X. Wei

School of Materials Science & Engineering, Beijing University of Aeronautics & Astronautics, Beijing 100191, China

(Received 09 June 2013; published online 02 September 2013)

Nanosized (10~50 nm) cathode material  $\text{Li}_2\text{MnO}_3$  was prepared for with  $\text{MnSO}_4 \cdot \text{H}_2\text{O}$ ,  $\text{KMnO}_4$  and  $\text{LiOH}$  aqueous solution as the precursor via single-step hydrothermal reaction by controlling the reaction time, proportion of processor, and the reagent concentration. The prepared materials were well crystallized and exhibited a monoclinic  $\text{Li}_2\text{MnO}_3$  structure with a space group of  $C2/m$  phase. The electrochemical performance of the material was tested at current density of  $60 \text{ mA g}^{-1}$  (1/4 C) between 4.3V and 2.0 V at room temperature, showing good electrochemical properties with the initial discharge capacity of  $243 \text{ mAh g}^{-1}$ , because it was more exposed to the electrolyte due to its nanostructure.

**Keywords:**  $\text{Li}_2\text{MnO}_3$ , Lithium manganese oxide, Hydrothermal Method, Nanostructure, Electrochemical Performance.

PACS number(s): 81.07. - b, 81.16.Be, 82.45.Yz

### 1. INTRODUCTION

Recently, as the electrochemical performances of electrode materials are greatly affected by the dimensionality and morphology of the material [1], nanostructured electrode materials have attracted great interest, and considerable effort has been paid to fabricate nanostructured Li-Mn-O electrode materials. Lithiated manganese oxides like the spinel-structured  $\text{LiMn}_2\text{O}_4$  and orthorhombic or mono-clinic structured  $\text{LiMnO}_2$ , are widely studied and can be used as positive electrodes in lithium batteries [2]. As promising candidates for cathode materials,  $\text{LiMn}_2\text{O}_4$  and  $\text{LiMnO}_2$  have the advantages of low cost, abundance and nontoxicity [3]. However,  $\text{LiMnO}_2$  tends to transform into a spinel structure during the lithium insertion/extraction process due to cation migration [4]. On the other hand,  $\text{LiMn}_2\text{O}_4$  suffers from capacity fading due to manganese dissolution [5] and the Jahn-Teller distortion [6, 7].

The structures of the lithium-rich layered materials are basically derived from the layered rock-salt  $\text{NaFeO}_2$  type structure with space group  $R\bar{3}m$ . Additional Li ions occupy the transition metal (TM) layers, which results in an additional superstructure with the honeycomb Li/Mn ordering in the end member compound  $\text{Li}_2\text{MnO}_3$  (alternatively described as  $\text{Li}[\text{Li}_{1/3}\text{Mn}_{2/3}]\text{O}_2$  in the layered notation). Layer-structured  $\text{Li}_2\text{MnO}_3$  is thermodynamically stable.

Self-seeding, surfactant-directed hydrothermal, sol-gel, and solid reaction methods were employed to synthesize Li-Mn-O nanostructures [8, 9, 10]. Within these, Wang et al. [10] synthesized single-crystalline  $\text{Li}_2\text{MnO}_3$  nanorods via a low-temperature molten salt synthetic route while no electrochemical performance was tested. Oxygen-deficient  $\text{Li}_2\text{MnO}_{3-x}$  ( $0 < x < 0.19$ ) was synthesized from lithium-rich manganese oxide,  $\text{Li}_2\text{MnO}_3$ , using metal hydrides ( $\text{CaH}_2$  and  $\text{LiH}$ ) as reducing

agents at reaction temperatures of 255-265 °C [11]. However, these methods suffered from either high temperature heat treatment or use of expensive reagents, and process complexity.

In this article, we obtained well-crystallized  $\text{Li}_2\text{MnO}_3$  nanoparticles by controlling the hydrothermal reaction time, proportion of processor, and the reagent concentration. The prepared materials delivered a high electrochemical reversible capacity charged/discharged between 2.0-4.3V.

### 2. EXPERIMENTAL

#### 2.1 Preparation and characterization of $\text{Li}_2\text{MnO}_3$

$\text{MnSO}_4$  and  $\text{KMnO}_4$  at a molar ratio of 4:1 were dissolved in distilled water. The concentration of  $\text{MnSO}_4$  was 0.01 M, and excess  $\text{LiOH}$  was added into the mixed solution, with the  $\text{LiOH}$  concentration of 0.32M. A brown suspension was immediately formed as soon as the  $\text{LiOH}$  was poured into the  $\text{MnSO}_4/\text{KMnO}_4$  solution. The mixed solution was then transferred to a Teflon-lined stainless steel autoclave for the hydrothermal reaction at 200 °C for 32 hours. Then, the obtained precipitate washed thoroughly with distilled water and dried at 60 °C in air.

X-ray powder diffraction (XRD) measurement was carried out using a  $\text{Cu K}\alpha$  radiation of Rigaku Rint2200 diffractometer. Morphology of the prepared powder was observed by a Hitachi H-8100 TEM (200 kV).

#### 2.2 Electrochemical measurements

The working electrodes was prepared by compressing a mixture of active materials, acetylene black, and binder (polytetrafluoroethylene, PTFE) at a weight ratio of 75:15:5. Lithium metal was used as the counter and reference electrodes. The electrolyte was  $\text{LiPF}_6$  (1M) in a mixture of ethylene carbonate (EC), dimethyl car-

\* liugr1108@gmail.com

† csc@buaa.edu.cn

bonate (DMC), and ethyl methyl carbonate (EMC) with a weight ratio of 1:1:1. All procedures for handling and fabricating the electrochemical cells were performed in an argon-filled glove box. The test cells were galvanostatic cycled between 4.3 and 2.0V vs Li at a current density of 60mA/g.

### 3. RESULT AND DISCUSSION

#### 3.1 Structures and Morphologies Analysis

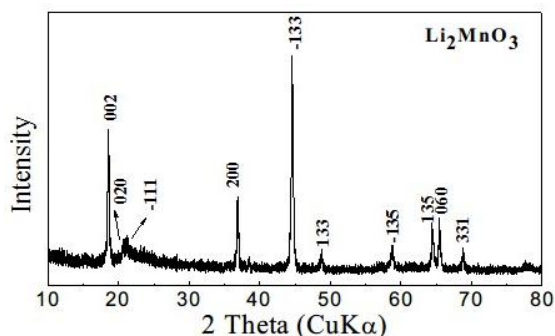


Fig. 1 – XRD patterns of nanostructured monoclinic  $\text{Li}_2\text{MnO}_3$  prepared at 200°C with the precursor  $\text{MnSO}_4$ ,  $\text{KMnO}_4$ , and  $\text{LiOH}$

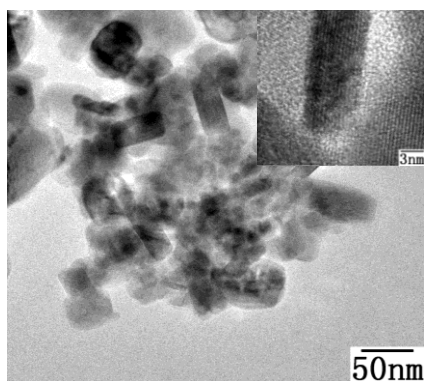
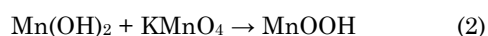


Fig. 2 – TEM images of the as-prepared layered  $\text{Li}_2\text{MnO}_3$  powders

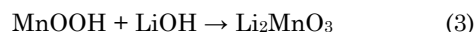
XRD patterns of hydrothermal products are shown in Fig. 1. All peaks of pattern can be indexed as monoclinic  $\text{Li}_2\text{MnO}_3$  structure with a space group of  $C2/m$  phase, which structure is the same as that of  $R3m$  layered rock-salt structures and none impurity phases were detectable in the products. Well-developed peaks in all synthesized materials at  $2\theta = 64.5^\circ$  and  $65.5^\circ$  corresponds (1 3 5) and (0 6 0) directions clearly remained, which indicated the degree of development of the monoclinic structure of  $\text{Li}_2\text{MnO}_3$ .

By adding  $\text{LiOH}$  into mixed solution of  $\text{MnSO}_4$  and  $\text{KMnO}_4$ , a precipitate of  $\text{Mn}(\text{OH})_2$  was formed immediately. The precursor  $\text{KMnO}_4$  was employed to oxidize  $\text{Mn}(\text{OH})_2$ , and the reaction route involving adding oxidant before lithiation is as follows:



$\text{LiOH}$  was the source of lithium ion in preparation of lithium manganese oxide and also affected the pH value. With lower content of  $\text{LiOH}$ ,  $\text{MnOOH}$  was further oxidized and formed into  $\text{Li}_2\text{MnO}_3$  phase, with manganese

value at +4. It can be summarized as follows:



Investigation showed that the ratio of  $\text{MnSO}_4/\text{KMnO}_4$  and the  $\text{LiOH}$  concentration were two key factors influencing the final product phase. In the hydrothermal system,  $\text{Mn}^{2+}$  in  $\text{MnSO}_4$  was oxidized by  $\text{KMnO}_4$  inevitably, therefore the proportion of  $\text{MnSO}_4/\text{KMnO}_4$  was important in decision of the value of Mn in production. On the other hand, the concentration of  $\text{LiOH}$  plays two important roles in the process, as the Li ion source to form orthorhombic Li-Mn-O by intercalation and as a reagent to regulate the pH value because the oxidibility of  $\text{KMnO}_4$  has significant impact on the pH value of the solution.

Typical TEM micrographs of  $\text{Li}_2\text{MnO}_3$  powder are shown in Fig.2. The final particle morphology is the mixture of nanorods and nanocube, with the size about 10 to 50nm. The high resolution transmission electron microscopy (HRTEM) imaging shows that the production is well crystallized.

#### 3.2 Electrochemical Properties

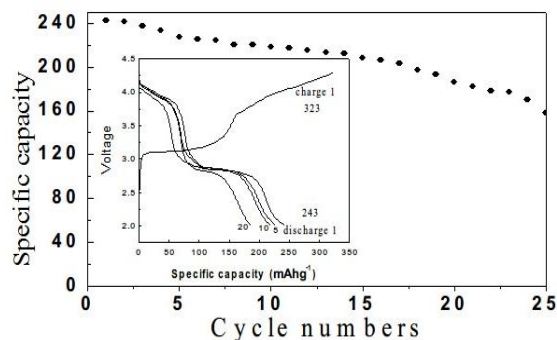


Fig. 3 – Cycling performance of as prepared  $\text{Li}_2\text{MnO}_3$  tested at current density of  $60\text{mA}\cdot\text{g}^{-1}$  between 4.3V and 2.0 at room temperature.

The electrochemical performance of  $\text{Li}_2\text{MnO}_3$  can be seen in Fig.3. The initial specific discharge capacity was  $243\text{mAh}\cdot\text{g}^{-1}$ . It is well-known that the stoichiometric  $\text{Li}_2\text{MnO}_3$  material commonly shows no electrochemical reaction in 4.5~2.0V [12,13], because its charge balance can be expressed as  $\text{Li}_2^+\text{Mn}^{4+}\text{O}_3^{2-}$ . It was reported that when  $\text{Li}_2\text{MnO}_3$  electrodes are initially charged to a high potential, typically  $>4.5\text{V}$  vs.  $\text{Li}^0$ , lithia ( $\text{Li}_2\text{O}$ ) is extracted from the  $\text{Li}_2\text{MnO}_3$  component in a combined electrochemical process (lithium removal) and chemical process (oxygen loss) before electrolyte oxidation [12], and on discharge, it is possible to reinsert lithium ion before the rocksalt  $\text{LiMnO}_2$  stoichiometry is reached [13]. In order to electrochemically activate  $\text{Li}_2\text{MnO}_3$  by removing  $\text{Li}_2\text{O}$  from the structure, it is necessary to charge  $\text{Li}/\text{Li}_2\text{MnO}_3$  cells to a high potential, typically  $>4.5\text{V}$  [14-16]. A more reasonable explanation has been advanced by Dahn et al. based on oxygen loss [17, 18]. The extra capacity to deliver Li could have important contribution for use of lithium manganese oxides in rechargeable lithium batteries. It was noted that on the initial charge to 4.5 V, only 20 mAh/g could be extracted from the  $\text{Li}_2\text{MnO}_3$  electrode. By charging to 5.0 V, a capacity equivalent to 383 mAh/g was obtained [13].

In our test, the  $\text{Li}_2\text{MnO}_3$  shows large specific capacity between 4.3 and 2.0V. This is attributed to the vicinity of the surface, or shallow reaction depth [19] (<50 nm) of the nanosized  $\text{Li}_2\text{MnO}_3$ . With nano-structured particle size, the specific surface of cathode particles was accordingly enlarged, leading to more  $\text{Li}_2\text{MnO}_3$  exposed to the electrolyte, then making it easier for  $\text{Li}_2\text{O}$  extracted from the  $\text{Li}_2\text{MnO}_3$  component. As a result, the surface electrochemical reactivity between electrolyte and electrode materials was greatly improved, finally improving the electrochemical properties [20].

By charging to 4.3 V, a charge capacity of 323 mAh/g was obtained. This corresponds to 70% of the theoretical value of  $\text{Li}_2\text{MnO}_3$  (459 mAh/g) when all the lithium ions are extracted. Complete removal of  $\text{Li}_2\text{O}$  from the  $\text{Li}_2\text{MnO}_3$  rocksalt structure leads to the formation of  $\text{MnO}_2$ . However, on discharge, it is possible to reinsert only one lithium ion before stoichiometric rocksalt  $\text{LiMnO}_2$  is formed. Therefore, the initial charge/discharge reaction of  $\text{Li}_2\text{MnO}_3$  cells can only be 75% coulombically efficient. With cycling, the efficient increased to 85% after 20cycles.

## REFERENCES

1. G.L. Che, B.B. Lakshmi, E.R. Fisher, C.R. Martin, *Nature* **393**, 683 (1998).
2. J.-M. Tarascon, M. Armand, *Nature* **414**, 359 (2001).
3. A.R. Armatrong, P.G. Bruce, *Nature* **381**, 499 (1996).
4. B. Amundsen, J. Paulsen. *Adv. Mater.* **13**, 943 (2001).
5. S.J. Wen, T.J. Richardson, L. Ma, K.A. Striebel, P.N. Ross, E.J. Cairns, *J. Electrochem. Soc.* **143**, L136 (1996).
6. M.M. Thackeray, Y. Shao-Horn, A.J. Kahaian, K.D. Kepler, E. Skinner, J.T. Vaughey, S.J. Hackney, *Electrochem. Solid State Lett.* **1**, 7(1998).
7. L. Croguennec, P. Deniard, R. Brec, *J. Electrochem. Soc.* **144**, 3323 (1997).
8. L. Zhang, J. Yu, A. Xu, Q. Li, K. Kwong, L. Wu, *Chem. Commun.* 2910 (2003).
9. X.D. Lian, W.S. Yang. *Solid State Ionics* **176**, 803 (2005)
10. X. Wang, J.M. Song, L.S. Gao, H.G. Zheng, M.R. Ji, Z.D. Zhang, *Solid State Commun.* **132**, 783 (2004).
11. K. Kubota, T. Kaneko, M. Hirayama, et al., *J. Power Sources* **216**, 249(2012).
12. J.S. Kim, C.S. Johnson, J.T. Vaughey, et al., *Chem. Mater.* **16**, 1996 (2004).
13. C.S. Johnson, J-S. Kim, C. Lefief, et al., *Electrochemistry Communications* **6**, 1085 (2004).
14. A. Robertson, P.G. Bruce, *Chem. Commun.* 2790 (2002).
15. P. Kalyani, S. Chitra, T. Mohan, S. Gopukumar, *J. Power Sources* **80**, 103 (1999).
16. A.R. Robertson, P.G. Bruce, *Electrochem. Solid State Lett.* **7**, A1 (2004).
17. M.N. Richard, E.W. Fuller, J.R. Dahn, *Solid State Ionics* **73**, 81 (1994).
18. Z. Lu, J.R. Dahn, *J. Electrochem. Soc.* **149**, 815(2002).
19. M. Tabuchi, Y. Nabeshima. *J. Power Sources* **174**, 554 (2007).
20. D.R. Rolison, B. Dunn, *J. Mater. Chem.* **11**, 963(2001).

## 4. CONCLUSIONS

Nanostructured  $\text{Li}_2\text{MnO}_3$  was successfully prepared via one-pot hydrothermal reaction using  $\text{MnSO}_4 \cdot \text{H}_2\text{O}$ ,  $\text{KMnO}_4$  and  $\text{LiOH}$  aqueous solution as the precursor at a low temperature at 200 °C. The cathode materials was tested between general 4.3 and 2.0V voltage window, and shows good electrochemical properties in rechargeable lithium batteries with the initial discharge capacity of 242 mAh  $\cdot$  g<sup>-1</sup>. The excellent electrochemical performances of as-obtained  $\text{Li}_2\text{MnO}_3$  nanoparticles indicated their promising future for application as cathode materials in lithium-ion batteries.

## ACKNOWLEDGEMENT

This work was supported by the National Basic Research Program of China (973 Program) (2013CB934000), National Natural Science Foundation of China (51074011 and 51274017) and National 863 Program (2007AA03Z231 and 2011AA11A257).